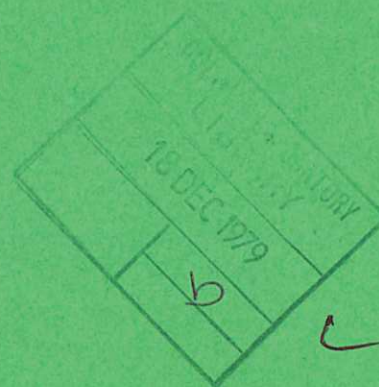


UKAEA

Preprint



REVIEW OF DITE WORK

J.W.M. PAUL

CULHAM LABORATORY
Abingdon Oxfordshire

1979

This document is intended for publication in a journal or at a conference and is made available on the understanding that extracts or references will not be published prior to publication of the original, without the consent of the authors.

Enquiries about copyright and reproduction should be addressed to the Librarian, UKAEA, Culham Laboratory, Abingdon, Oxon. OX14 3DB, England.

Invited Paper
9th European Conference
on
Controlled Fusion and Plasma Physics
Oxford, September 1979

REVIEW OF DITE WORK

J.W.M. Paul

Culham Laboratory, Abingdon, Oxon, OX14 3DB, UK
(EURATOM/UKAEA Fusion Association)

ABSTRACT

The behaviour of the DITE tokamak, including LMW injection and the bundle divertor, is reviewed with particular emphasis on MHD activity.

October 1979

REVIEW OF DITE WORK

by

J.W.M. Paul

Culham Laboratory, Abingdon, Oxon, OX14 3DB, UK
(Euratom/UKAEA Fusion Association)

ABSTRACT: The behaviour of the DITE tokamak, including both 1 MW injection and the bundle divertor, is reviewed with particular emphasis on MHD activity.

1. INTRODUCTION

Aims: This paper attempts to place the seven contributed papers and some more recent work on DITE into a more general context. The aims of the DITE programme are largely the same as previously, but can now be grouped as activities;

- (a) Leading up to and supportative of JET, from plasma physics to diagnostics.
- (b) Testing the longer term attractiveness of the bundle divertor for exhaust and control of impurities in the next generation of machines (e.g. TIGER/INTOR).

Both of these activities involve understanding (i) the origin, role and control of impurities and MHD activity and (ii) the physical processes involved in a tokamak dominated by injection heating.

Physics Progress: Five main points can be listed;

- 1) The injection of 1 MW of neutral beam power to the plasma has tripled the ion temperature to 1 keV and indicated, but not proved, the presence of the beam driven current. The injection work has also revealed some problems of interpretation.
- 2) Low q discharges are run routinely with $q = 2.2$ for 0.1 s without deterioration of containment.
- 3) The combination and comparison of diversion and gettering shows that diversion further reduces both low and high Z impurities in a gettered torus.

- 4) Injection into a diverted discharge has doubled the ion temperature in some preliminary experiments.
- 5) In all the above work MHD activity plays an important role particularly with clean plasmas. The activity is variable and its origin is not understood but it seems to point to the need for a better understanding of the initial phase of the discharge.

Technological Progress: The last E.P.S. review of DITE work concluded that pure plasmas with auxiliary heating were required. We demonstrated the effectiveness of gettering and the bundle divertor to achieve the former, and neutral injection for the latter. Since then we have, and are continuing, to upgrade both injection and divertor systems. The first main technological achievement has been upgrading the injection system to 1 MW to the plasma (Paper AP3), with average reliability of 85% and 100% for single days. Next year this system will be replicated to provide 2 MW. The second achievement is the design of a new bundle divertor (Mk II) for operation at full field (2.8 T) on DITE and this design has greater potential for reactors. The Mk II divertor is under construction and will be installed next year. In the meantime the Mk I has been upgraded to 1.5 T but is operational at 1.0 T at present.

Like most other major tokamaks, there have been technical problems with our machine, in particular with the toroidal and divertor field systems and with the long commissioning of the injection system. While these have severely reduced experimental time, the problems have largely been overcome. However, viewing the whole fusion community, the implementation of technology needs to be improved so that more machines operate on design performance, on time and most of the time. Such an improvement in reliability would also improve the credibility of the advance to a reactor.

Diagnostic Progress: Apart from improving more standard diagnostics, we have developed a technique for measuring, for the first time, the four Stokes parameters which define properly the polarisation of the electron cyclotron emission (Paper EP13). Studies of the latter, pioneered at Culham Laboratory with the NPL, have now become an extremely convenient method of measuring $T_e(r)$ (Paper EP12).

Although the measurements usually agree with other data, the physical processes and the errors need to be better understood or

documented. This new technique should help. The problems appear to lie in the variability of the polarisation, similarity of spectra from radial, vertical and tangential directions, calibrations and the fact that it appears to work even when the plasma should be optically thin.

DITE Experiment: The layout of DITE is shown in Fig. 1, and the parameters are listed below:

Tokamak:

$$r_L = 0.26 \text{ m} ; R = 1.17 \text{ m}$$

$$I_g \lesssim 280 \text{ kA} ; B_T \lesssim 2.7 \text{ T}$$

Limiters:

Mo limiters, recently changed to Ti and/or C.

Injection:

$$P_{inj} \lesssim 1.1 \text{ MW}; V \lesssim 28 \text{ kV} \quad t \lesssim 50 \text{ ms}$$

Divertor:

$$I_g \lesssim 75 (100) \text{ kA}, B_T \lesssim 1.0 (1.5) \text{ T}$$

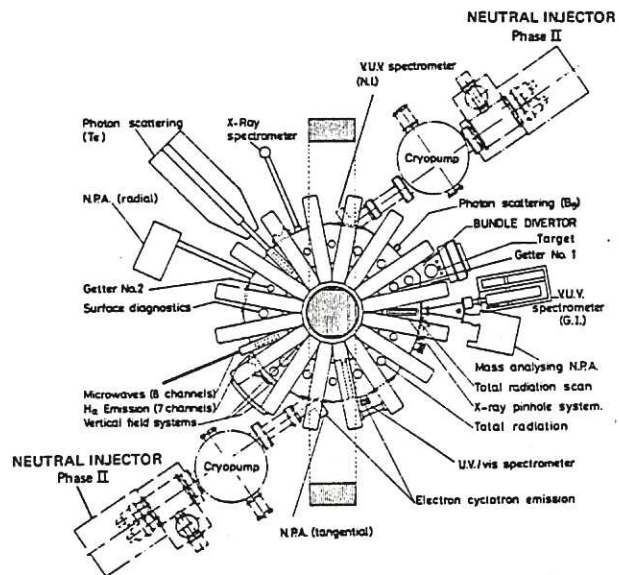


Fig. 1. Schematic layout of DITE.

2. TOKAMAK

2.1 Introduction

For the discussion which follows, two simple diagrams should be useful. The first (Fig. 2) is a schematic $T_e(r)$ which illustrates three regions of the plasma, namely the central core, the intermediate and the boundary layer. These are separated by the 'natural' boundaries of the $q = 1$ and $q = 2$ surfaces respectively. The MHD activity at each of these surfaces can permeate the adjacent regions and dominate plasma behaviour. The structure provides the matching of the hot plasma to the cold wall. The second (Fig. 3) is the Hugill operating diagram which illustrates how tokamaks are boxed in by MHD activity leading to disruption.

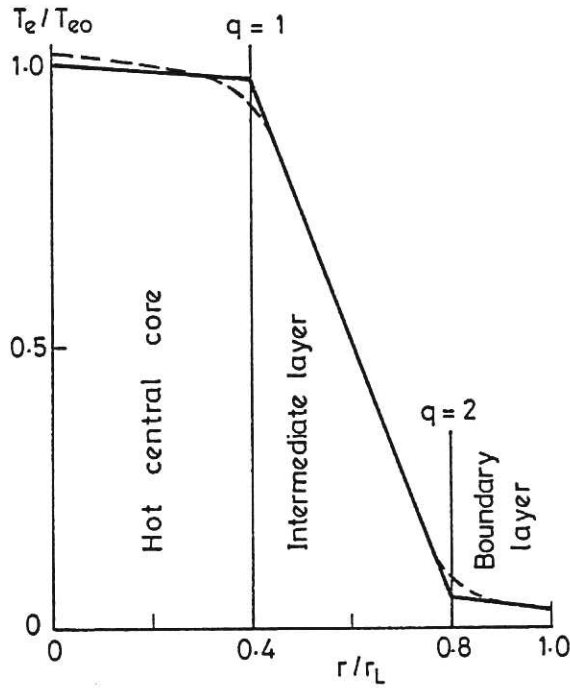


Fig. 2. Schematic plasma structure.

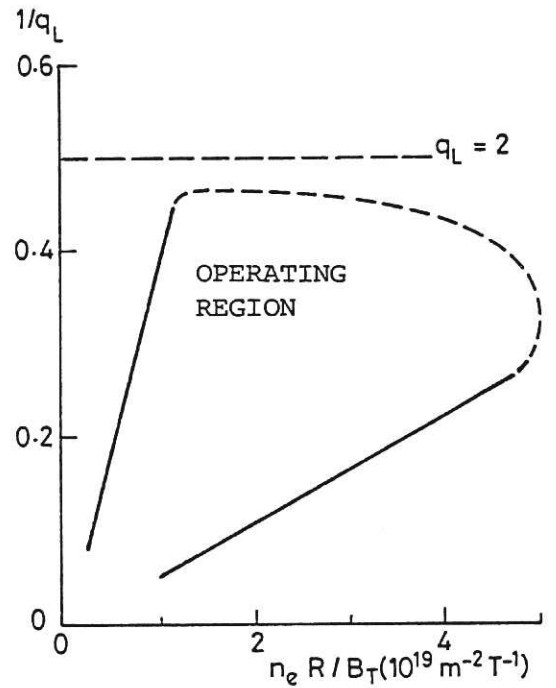


Fig. 3. Schematic operating region.

2.2 Plasma Structure

Boundary Layer: Through this layer, plasma is fuelled with hydrogen, from the walls and the gas feed, and with impurities from the walls. Low Z impurities arise mainly from desorption, while high Z impurities arise from arcs (not necessarily unipolar) and/or sputtering. The emission from hydrogen (H_α) and lowly ionised impurities (eg O II), which tends to be largely from this region, is often asymmetric in major and minor azimuth. The level of $m = 2$ MHD activity, originating at the $q = 2$ surface, appears to have an important influence on fuelling (c.f. § 2.3).

Langmuir probe measurements show (a) the ratio of average edge density at the limiter to \bar{n}_e is about 0.1, but is lower with gettered walls or with the divertor on, (b) an edge T_e which falls with increasing n_e and this is probably related to the reduced arcing/sputtering at high n_e and (c) fluctuations which vary from 8% to 100%. As yet, these fluctuations have not been correlated with other parameters such as MHD activity around the $q = 2$ surface or the influx of impurities.

This region of the plasma is of particular interest because it forms the scrape-off layer for the bundle divertor.

Intermediate Layer: This layer matches the hot core to the cold boundary by providing the main containment. Within the layer the electron thermal conductivity (anomalous) increases with radius. The ion thermal conductivity is normally between 1 and 10 times neoclassical (typically 5 on DITE).

Under certain conditions MHD activity, namely the $m = 2$ mode at $q = 2$ and the sawtooth at $q = 1$, can influence the matching process.

Hot Central Core: With Mo limiters the core is radiation cooled with a peak radiation profile, $P_{\text{rad}}(r)$. This results in a tendency for $T_e(r)$ to be hollow.

With Ti or C limiters $P_{\text{rad}}(r)$ is lower and almost flat, while T_e is higher. The sawteeth at $q = 1$ are now more important in both the energy and particle transport. For low $q \sim 2.2$, this central core can extend to half the radius.

2.3 Operating Diagram (Fig. 4)

High Density Limit: With gettered walls, direct local fuelling by externally controlled gas feed is dominant although fast neutrals are still recycled by the walls. In this situation the H_α emission would need to be resolved in three dimensions to represent the fuelling and neutral density. The evolution of impurities is reduced along with the recycling, but it is believed that even in a 'pure' plasma the density is still limited by impurity cooling of the edge. When the divertor can be operated at higher density, with more effective screening (now only 50% for oxygen), it should extend the density limit appreciably. This limit has already been extended by the application of neutral injection heating.

At the last E.P.S. Conference we reported pauses in a rising density associated with changing profiles which had some associated MHD activity. Now we have clear evidence that the effectiveness of gas feed for increasing the density is impaired, when the $m = 2$ activity is high (wall $\Delta B_p/B_p \sim 1\%$). The two pulses in Fig. 5 have identical gas feed rates but show markedly different density behaviour because of the difference in MHD activity. This suggests that the initial stage pre-determined this MHD level and therefore the subsequent behaviour.

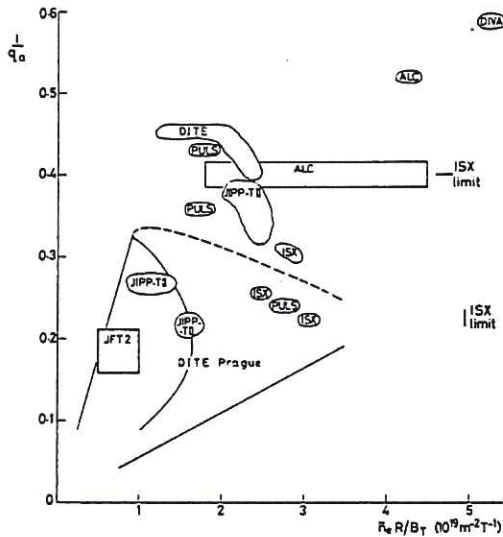


Fig. 4. Hugill diagram.

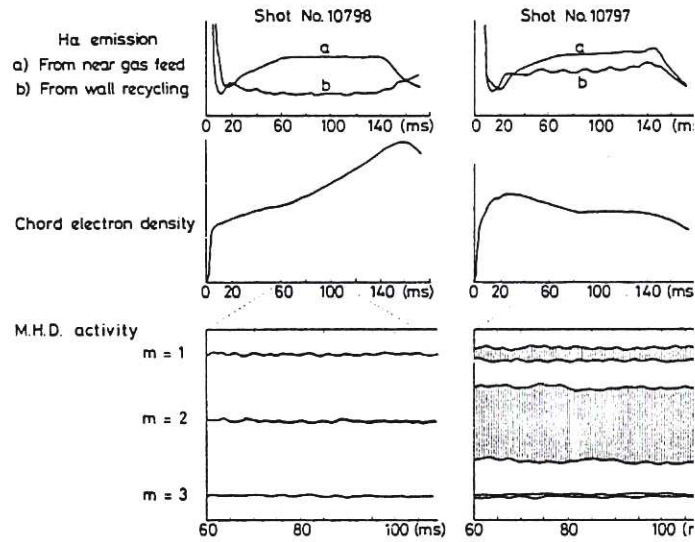


Fig. 5. Gas feed and M.H.D. activity.

Low q Operation: This offers a larger central core and higher β_T . In particular on DITE it should allow operation of the Mk IB divertor at higher currents and densities for neutral injection experiments. Discharges with $q = 2.2$ have been maintained for 100 ms without any disruptions (Paper EP11). This is easier to achieve with Ti limiters and gettering ($Z_e \sim 1$) and when $m = 2$ activity is low. Typical profiles for a discharge with $q = 2.2$ are shown in Fig. 6. There is no appreciable deterioration in the energy containment time with this reduced q .

There is a pause in the rising density (Fig. 7), corresponding with enhanced $m = 2$ activity, as the current passes through $q_L = 3$. With a more steady but lower density the current passes through $q = 3$ with a burst of MHD activity (Fig. 8) but without a density pause. The density was raised later, with $q = 2.2$, by increasing the gas feed.

An attempt to break the $q = 2$ barrier on DITE (no copper shell) normally resulted in disruption at $q = 2$ but on the one occasion when $q \sim 1.6$ was achieved, it resulted in a violent terminal disruption with internal damage to the machine.

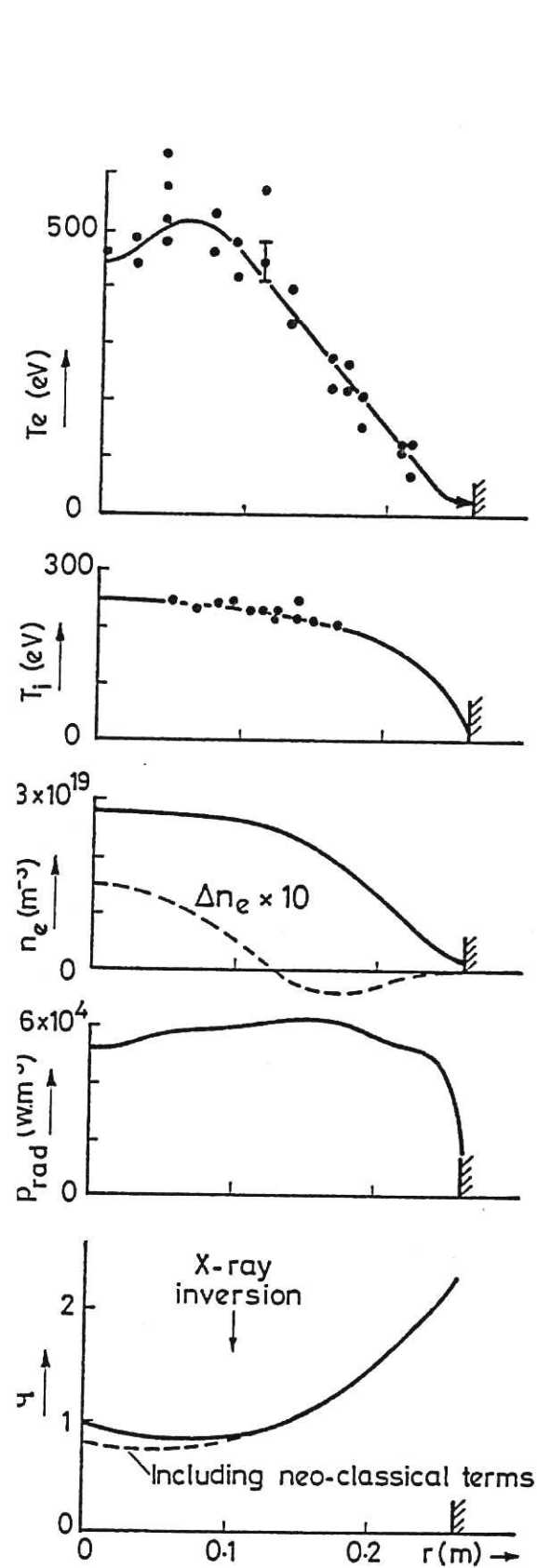


Fig. 6. Radial profiles at low q .

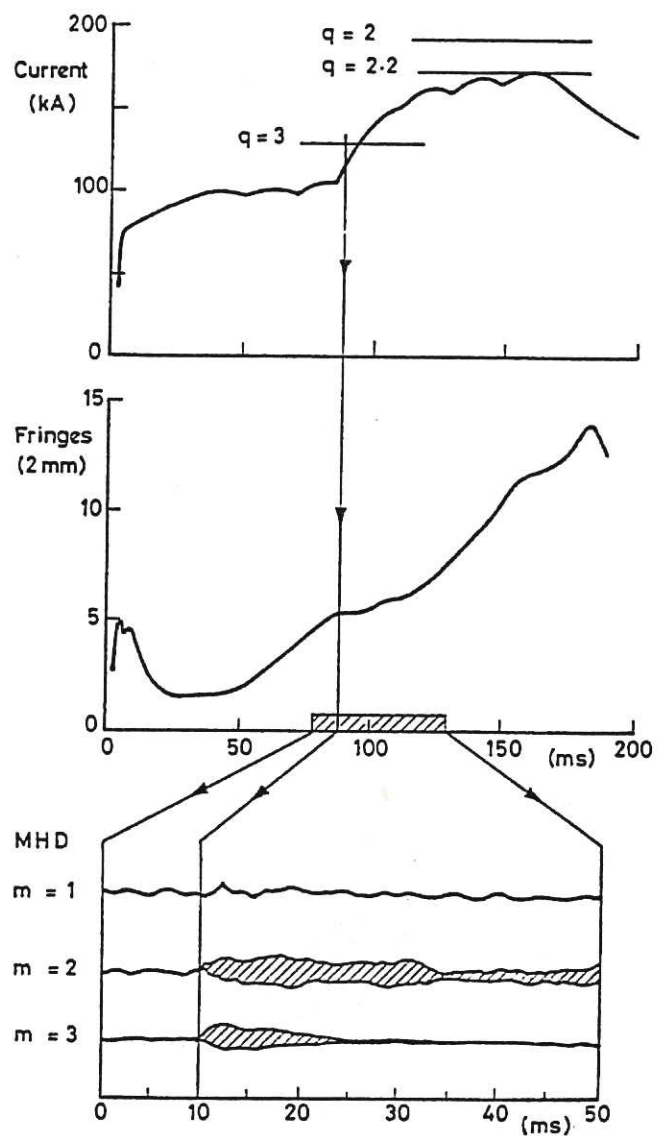


Fig. 7. Low q oscillograms (n_e pause).

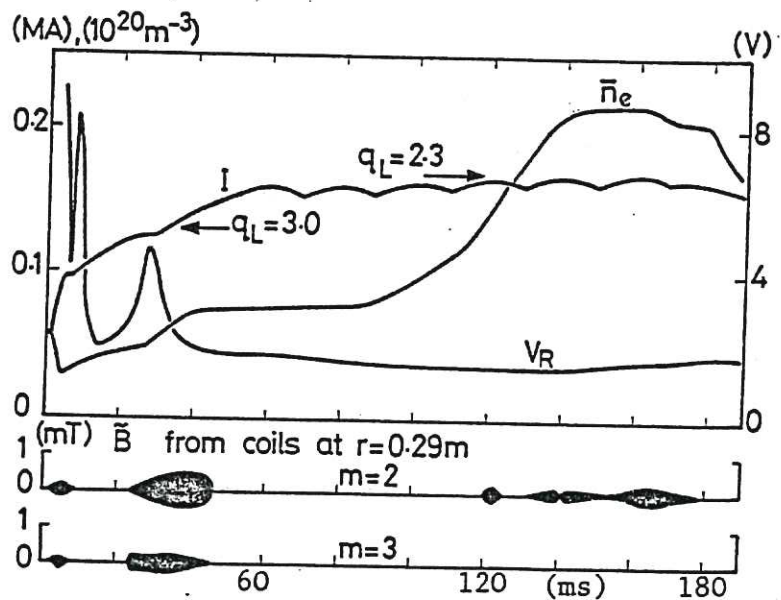


Fig. 8. Low q oscillograms.

3. PLASMA DECAY EXPERIMENT

In a gettered torus, switching off the gas feed gives rise to a rapid decay of density to a low plateau. The decay time, which is about 20 ms for a wide range of densities can be related to a particle containment time of about 15 ms, taking account of particle reflections. However, the density profiles change appreciably during the decay (Fig. 9) and analysis, assuming no recycling but correcting for the neoclassical pinch, gives a diffusion coefficient

$$D \sim \frac{0.5 \times 10^{19}}{n_e} \text{ m}^2 \text{ s}^{-1}$$

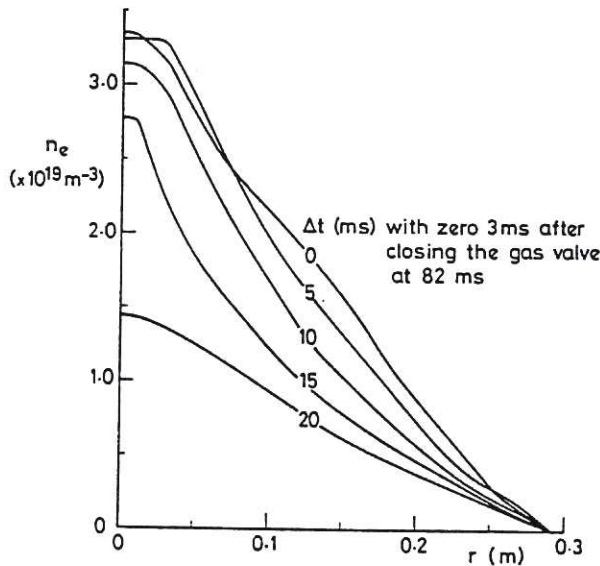


Fig. 9. Density decay profiles.

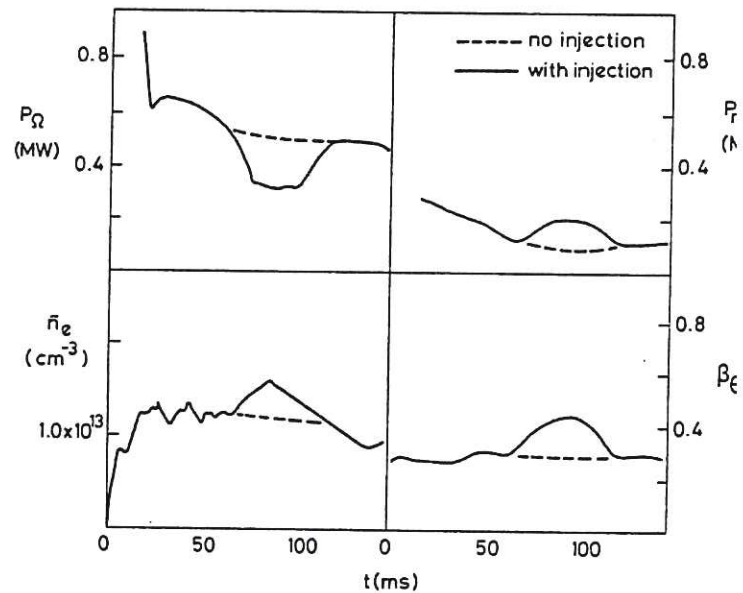


Fig. 10. Injection oscillograms.

4. INJECTION

4.1 Objective

The main objective of the DITE injection programme has been to achieve high ion temperatures rather than high β . At Culham Laboratory the latter is one of the main aims of the Tosca programme. The maximum ion temperature achieved is 1 keV, about three times the initial value. However, without optimisation values of $\hat{\beta}_T = 1.5\%$ have been achieved (Paper EP9).

4.2 Mo Limiters

With Mo limiters injection usually induces MHD activity resulting in soft disruptions. There is a large increase in the radiated

power (Fig. 10) and no change in the electron temperature. In Fig. 11 a plot of ΔT_i against P_{inj}/n_e shows saturation at an ion temperature around 0.8 keV.

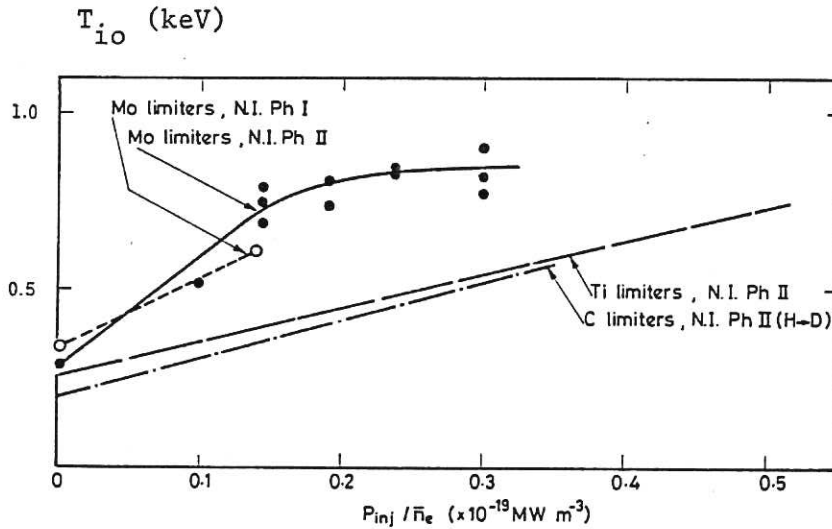


Fig. 11. Injection heating vs power.

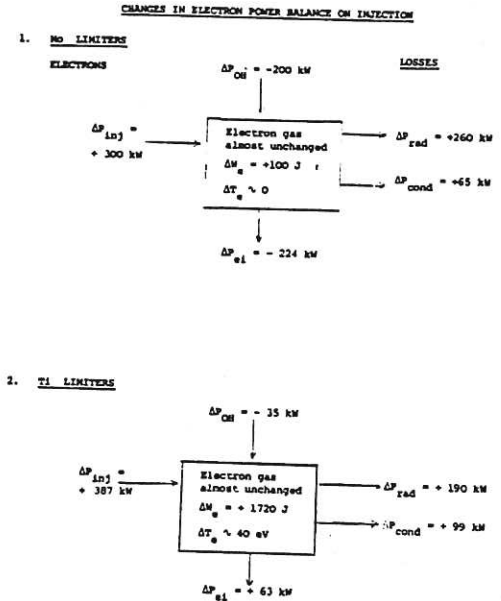


Fig. 12. Changes in electron power balance.

Power balances for the electrons and the ions show that with $T_i > T_e$ the electrons are acting as a thermostat. The temperature setting of the thermostat is presumably determined by the temperature dependence of the radiated power from a dominant impurity. The change in the electron power balance on injection is shown in Fig. 12. The ion power balance results in an ion thermal conductivity, $K_i = (5 \pm 2)K_{NC}$, as shown in Fig. 13.

The central O VII emission increases on injection more than the edge O II emission although $\Delta T_e \sim 0$. The corresponding increase in O II may be localised elsewhere but has not been found. Alternatively oxygen might be injected with the beam but its absence on a test rig makes this unlikely. Finally the beam charge-exchange on oxygen might be directly exciting the O VII emission.

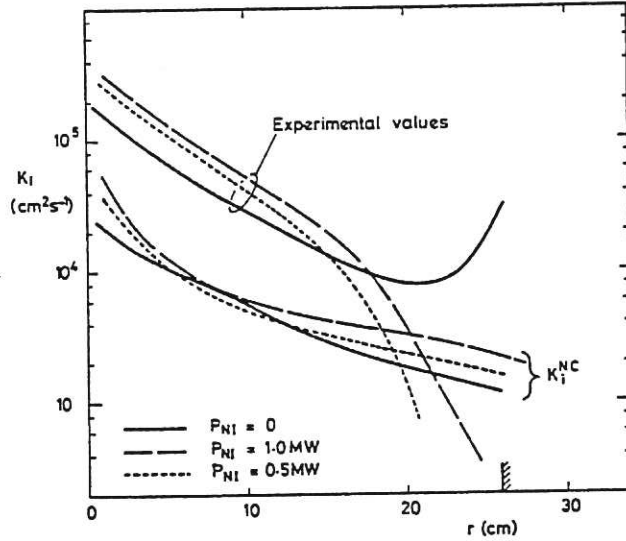


Fig. 13. Experimental and theoretical ion thermal conductivities.

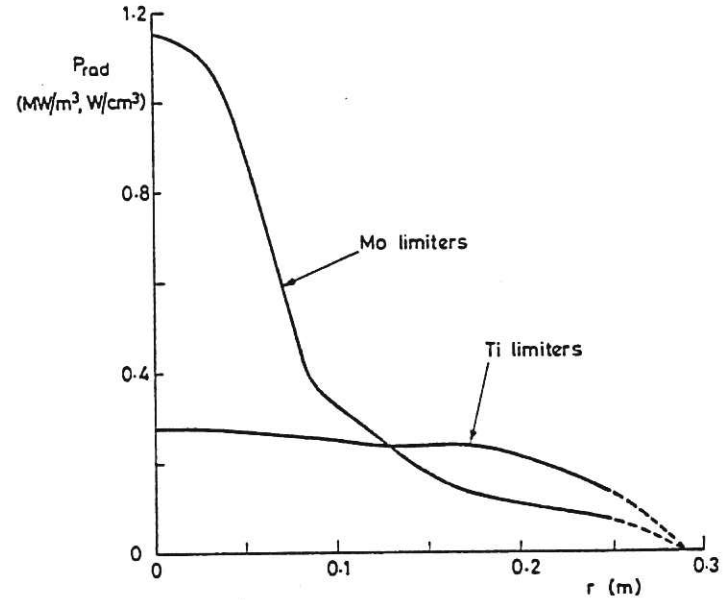


Fig. 14. Effect of limiter material on $P_{rad}(r)$ during injection

4.3 Ti and C Limiters

These more recent conditions have lower MHD activity and injection no longer induces disruptions. The total radiation and its increase on injection are lower (Fig. 14) and under some conditions T_e increases appreciably. As $T_e > T_i$ the electrons can no longer act as a thermostat. Now injection induces large density and X-ray sawteeth around $q = 1$ (Fig. 15). The period does not fit a simple 'overheating' model and at present we have no satisfactory model.

The plot of ΔT_i vs P_{inj}/n_e is now linear but lower (Fig. 11). Power balances for these discharges are not complete but there are indications that charge-exchange losses may be important. There are difficulties in obtaining representative experimental measurements of the neutral density. This is now appreciably localised at the gas feed and differently averaged by the circulating beam and the plasma ions.

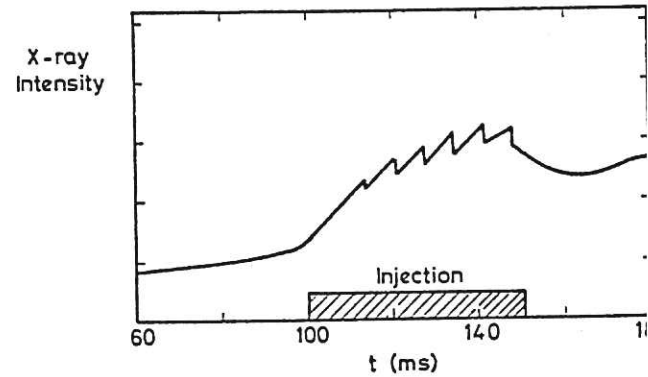


Fig. 15. Beam induced sawteeth

4.4 Beam Refuelling?

For the conditions of these experiments most of the injected beam is trapped by charge-exchange. The resulting hot thermal neutrals can be expected to move away several cm from their point of origin before ionisation or further charge-exchange. In some discharges the density rises smoothly without any sawteeth and the profile of density increase follows closely the deposition profile (Fig. 16). In the presence of sawteeth, (Fig. 17), they are equivalent to an outward flux of particles of magnitude roughly equal to that of the beam input. These equivalences may be fortuitous and are difficult to check without reliable 3-D measurements of the ionisation rate from H_{α} emission particularly in the localised region of beam deposition.

If the measured increase in density of injection resulted from ionisation of neutrals, then the required neutral density would give adequate charge-exchange losses in some discharges to explain the low ion temperatures.

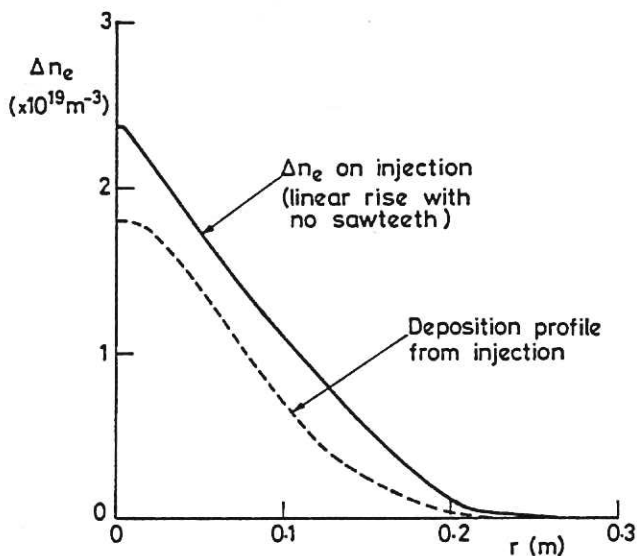


Fig. 16. Density rise on injection.

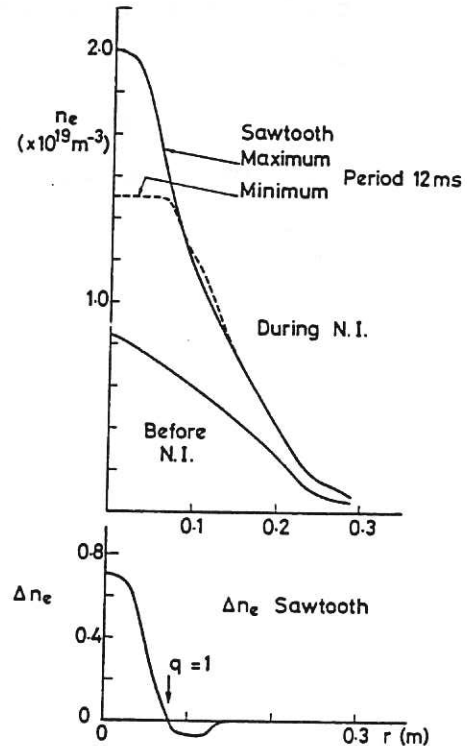


Fig. 17. Density sawteeth on injection.

4.5 Beam Induced Current?

With limiters of Mo there is no change in the electron temperature but a dramatic drop in the loop voltage. The drop in Ohmic power input in Fig. 10 is entirely due to a decrease in the voltage by about one third. This drop is comparable with that to be expected from the beam driven (Ohkawa) current. However, there should be an additional component caused by the plasma rotation which rough estimates suggest should be comparable.

With limiters of titanium the voltage often drops with an overshoot as shown in Fig. 18. Such behaviour is predicted as magnetic field transfers from the Ohmic to the beam driven current but the time scales appear shorter than predicted. However, in these experiments the electron temperature did change and a detailed analysis is required to demonstrate whether this could account for the voltage behaviour.

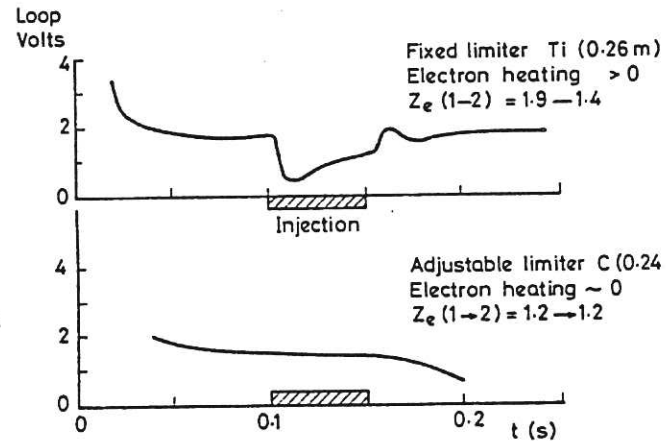


Fig. 18. Change in loop volts on injection.

With limiters of carbon the Z_{eff} is lower and there is negligible change in the loop volts on injection. The beam driven current should decrease with Z_{eff} but a more quantitative treatment is required.

These results are tantalizing in that they indicate the presence of a beam driven current, which cannot yet be demonstrated conclusively.

4.6 Conclusions on Injection

In DITE, with limiters of Mo the injection heating is limited by radiative power losses, while with limiters of Ti or C it may be limited by charge-exchange losses. The various injection experiments on DITE have been compared using a rough consumer figure of merit

$$M = \Delta(n_i T_i) / P_{inj} \sim \Delta(n_e T_i) / P_{inj}$$

where the numerator represents the desired product and the denominator the cost. For interest we extend this data (Table I) to include other experiments and added a volume correction ($M' = MV$).

TABLE I

CRUDE FIGURES OF MERIT FOR INJECTION

Machine	Ref	R (m)	a (m)	B _T (T)	I _g (kA)	Limiter	Gas	\bar{n}_e (2) (10^{19} m^{-3})	Z _{eff}	P _{inj} (kW)	V _b (kV)	T _{eo} (1-2) (eV)	T _{io} (1+2) (eV)	$\Delta(\bar{n}_e T_i)/P_{inj}$	$\Delta(\bar{n}_e T_i) v/P_{inj}$ (ms)
DITE	B	1.17	0.27	2.0	150	Mo	H	1.4	3.7	200	28	450	340 → 610	1.9	5.1
DITE	P	1.17	0.27	2.7	190	Mo	H	2.5	7.6	200	30	1000	540 → 640	1.3	3.5
DITE	P	1.17	0.27	2.0	150	Mo	H	2.1	6.8	200	30	845	440 → 660	2.3	6.1
DITE	OX	1.17	0.26	2.0	150	Mo	H	1.6	5	800	24	650	300 → 850	1.1	2.7
DITE	OX	1.17	0.26	2.0	145	Ti	D	2.2	4	750	24	930 → 970	200 → 560	1.4	3.5
ORMAK	B	0.8	0.23	2.5	175	W	H	2.8	7.9	360	30	1530 → 760	650 → 1830	9.1	12.1
TFR	B	0.98	0.20	6.0	360	Mo	H	5.6	2.8	400	39	1800	1200 → 1600	7.7	9.4
T11	B	0.70	0.18	1.0	110	Mo	D	2.0	-	280	20	650	300 → 500	1.4	0.96
T11	I	0.70	0.18	1.0	100	Mo	D	1.4	-	140	21	400 → 530	150 → 400	2.5	1.76
ISX-B	OR	0.92	0.27	1.2	115	St	H	2.0	-	300	40	800	350 → 700	2.3	4.8
ISX-B	OR	0.92	0.27	1.2	115	St	D	7.0	1.2	500	40	600 → 900	400 → 800	8.0	16.9
PLT	I	1.32	0.40	4.0	~400	C	H	2.0	2.5	2100	40	~3000	1000 → 6000	4.8	7.7

B = Berchtesgaden, P = Prague, I = Innsbruck, OR = Oak Ridge, OX = Oxford

There is no reason to expect M or M' to be constant in Table I but a systematic explanation of the large variation (~ 10) might be useful. There has been a systematic study of Ohmically heated tokamaks resulting in the creation of data banks and empirical scaling laws. Injection heated tokamaks are more complicated both experimentally and theoretically and in that codes and data need to be interleaved. The common statement, that injection heating is well understood, is probably true but needs careful checking because small factors on large machines cost large amounts of money.

The figure of merit takes no account of the scaling of transport processes (eg $M' \propto a^2$) but most experiments have similar dimensions (except PLT), similar currents (except PLT and TFR) and similar densities (except TFR and the high performance ISX-B). There is a tendency for high values of a , I and n_e to give good performance. However, ORMAK has a surprisingly high figure of merit, although the electrons are cooled. The magnitude of ΔT_e and Δn_e in injection experiments, is not always well understood.

The many factors involved in injection experiments can be classified:

- (1) target plasma; its basic parameters (r , I , n_e , T_e , T_i , T_e/T_i , n_i) and its impurity level (Z_{eff} , P_{rad} , n_i/n_e),

- (2) the beam, (E_b , species, impurity content, direction),
- (3) beam induced, (a) impurities, (b) radiated power, (c) fuelling or in some cases apparent defuelling, (d) toroidal current, (e) rotation, (f) MHD activity.

Three problem areas deserve mentioning, (i) the accuracy of the measured/calculated neutral density and refuelling, (ii) the presence or otherwise of the beam driven and rotational currents and (iii) the accuracy of the ratio K_i/K_{NC} , which varies by up to a factor of ten, when it is derived from subtracting large quantities.

5. BUNDLE DIVERTOR

5.1 General

We have only recently returned to a major programme on the bundle divertor. There are many modes of operation involving gettering, injection, mid-pulse switching and varying ratio I_{DIV}/I_{TOR} . The initial dirty discharges provided a dramatic illustration of the effect of the divertor on the plasma wall interactions in that repeated major disruptions were reduced to minor ones or removed altogether.

5.2 Gettering

The results reported at Prague and some preliminary experiments with gettering at that time, have been repeated. The comparison of gettered and ungettered cases, is shown in Fig. 19 (Paper EP8). These discharges have typically $I_g \sim 50$ kA, $T_{eo} \sim 300$ eV, $n_e \sim 10^{19} \text{ m}^{-3}$, $q_{sep} \sim 2.5$. The density drop on diversion is less with gettering because more of the fuelling is directly from the gas feed (hydrogen screening efficiency low ~ 0.2) rather than the walls. This refuelling data fits the DITE global recycling model. The screening efficiency for oxygen is the same in both cases (0.5) showing

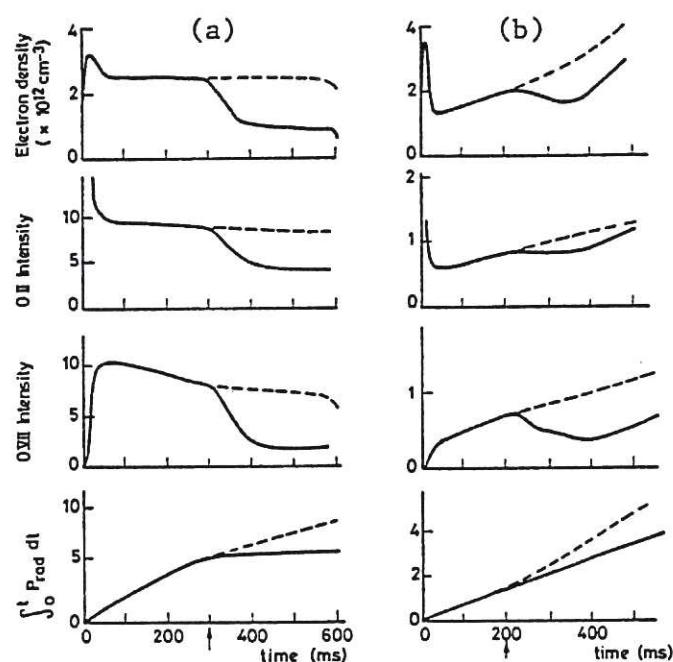


Fig. 19. Diversion without (a) and with (b) gettered walls.

that the divertor further reduces the low Z impurities in a gettered torus. The X-ray anomaly factor for the gettered discharge decreases on diversion by a factor of 4 to a value near unity (Table II) illustrating the further reduction of high Z impurities by the divertor.

Table II: X-Ray Anomaly Factors

<u>Divertor</u>	<u>Ungettered</u>	<u>Gettered</u>
Off	400	4.2
On	80	1.0

Higher densities ($\sim 2 \times 10^{19} \text{ m}^{-3}$) and currents ($\sim 75 \text{ kA}$) have been achieved with the divertor on but not yet reproducibly. Operation at higher density is important for obtaining better screening of low Z impurities. According to the standard model of the density limit, this should enable even higher densities to be achieved.

5.3 Instability

With increasing current or decreasing I_D/I_T , an instability sets in with a sharp threshold. The instability is observable on the loop volts, MHD coils, H_α and emission from outer (eg O II) but not inner (eg OVII) impurity states. There is still screening and power exhaust to the target. The phenomena appears to be associated with the presence of the $q = 2$ surface near the divertor separatrix, but this cannot be confirmed until more detailed measurements are made. The behaviour is variable but in one clear case the MHD $m = 2$ signal grows without rotation, presumably fixed by the divertor asymmetry, and drives a density sawtooth with reversal around the expected position of $q = 2$. A simultaneous break in the $m = 2$ growth and the sawtooth is accompanied by $m = 1$ activity, increased spectroscopic emission and increased voltage. The plasma appears to spill out like a minor disruption. The energy confinement time is appreciably reduced.

6. DIVERTOR WITH INJECTION

6.1 Heating

After preliminary experiments in 1977, we returned to this subject recently by injecting 200 - 450 kW at 16 keV into a discharge with a lower ratio $I_D/I_T = 1.5$ to obtain higher current $I_g = 60 \text{ kA}$. The beam transmission was about 20% and large charge-exchange and orbit losses can be expected. The ion temperature was observed to double to 200 eV,

demonstrating power transfer to the plasma. For the electrons $\Delta T_e \sim 0$ with $T_e \sim 400$ eV. Deposition and power balances have not yet been performed but there was no deleterious effect of diversion.

6.2 Diversion

The increase in the central radiated power on injection is decreased by the divertor as shown in Fig. 20. The behaviour of the impurity emission on injection (Fig. 21), which was reported in § 4.2, precludes the measurement of screening efficiency with injection.

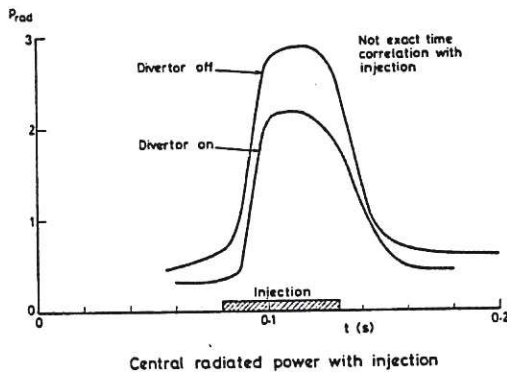


Fig. 20. Central radiated power on injection with and without diversion.

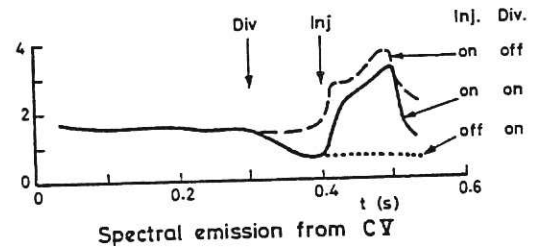


Fig. 21. Spectral emission from C V with and without diversion

7. CONCLUSIONS

We report two new results (i) the combination of diversion and injection and (ii) the importance and variability of MHD activity. These promise a fruitful period of research.

8. ACKNOWLEDGEMENTS

The author wishes to acknowledge but not 'incriminate' his colleagues on DITE, particularly Drs J. Hugill, R.D. Gill, A.J. Wootton, S.J. Fielding, R.S. Hemsworth, W.H.M. Clark, D.J. Campbell, P.E. Stott (now on JET) and G. Proudfoot.



